

Dry sediment loading of headwater channels fuels post-wildfire debris flows in bedrock landscapes

Roman A. DiBiase^{1,2*} and Michael P. Lamb³

¹Department of Geosciences, Pennsylvania State University, University Park, Pennsylvania 16802, USA

²Earth and Environmental Systems Institute, Pennsylvania State University, University Park, Pennsylvania 16802, USA

³Division of Geological and Planetary Sciences, California Institute of Technology, Pasadena, California 91125, USA

ABSTRACT

Landscapes following wildfire commonly have significant increases in sediment yield and debris flows that pose major hazards and are difficult to predict. Ultimately, post-wildfire sediment yield is governed by processes that deliver sediment from hillslopes to channels, but it is commonly unclear the degree to which hillslope sediment delivery is driven by wet versus dry processes, which limits the ability to predict debris-flow occurrence and response to climate change. Here we use repeat airborne lidar topography to track sediment movement following the 2009 CE Station Fire in southern California, USA, and show that post-wildfire debris flows initiated in channels filled by dry sediment transport, rather than on hillsides during rainfall as typically assumed. We found widespread patterns of 1–3 m of dry sediment loading in headwater channels immediately following wildfire and before rainfall, followed by sediment excavation during subsequent storms. In catchments where post-wildfire dry sediment loading was absent, possibly due to differences in lithology, channel scour during storms did not occur. Our results support a fire-flood model in bedrock landscapes whereby debris-flow occurrence depends on dry sediment loading rather than hillslope-runoff erosion, shallow landslides, or burn severity, indicating that sediment supply can limit debris-flow occurrence in bedrock landscapes with more-frequent fires.

INTRODUCTION

Sediment yields following wildfire commonly greatly exceed background erosion rates (Moody et al., 2013), threatening life and property at the wildland-urban interface in mountainous terrain (Cannon and DeGraff, 2009). Predicting the magnitude of this increase in sediment yield and the consequences of wildfire for longer-term landscape evolution requires a mechanistic understanding of how sediment is delivered from hillslopes to channels and the degree to which post-wildfire erosion is limited by hillslope sediment supply (Roering and Gerber, 2005; Lamb et al., 2011).

In landscapes continuously mantled in soil, post-wildfire sediment yield is governed primarily by rainfall (Gartner et al., 2014). That is, predominantly wet processes such as rilling (Wells, 1987), shallow landsliding (Gabet, 2003), and excavation of existing channel deposits (Santi et al., 2008) supply the bulk of sediment delivered to downstream channel networks and are the source of debris flows. Consequently, the

spatial pattern of post-wildfire erosion is thought to depend largely on the pattern of individual storms and the pattern of burn severity, which affects soil hydrophobicity and the degree of runoff erosion on hillslopes (Doerr et al., 2009; Parsons et al., 2010). In this model, the more-frequent fires predicted over the next century due to climate change (Westerling and Bryant, 2008; Mann et al., 2016) should lead to increased sediment yields and hazards because of the assumed inexhaustible supply of hillslope soil. However, it is unclear if these ideas developed for soil-mantled hillslopes also apply to steep, bedrock-dominated landscapes.

In landscapes where slopes are steeper than the angle of repose, sediment is transported dry from hillslopes to channels immediately following a wildfire by rolling and bouncing downslope by gravity alone (i.e., dry ravel) due to incineration of vegetation dams that temporarily trap soil (Krammes, 1965; Florsheim et al., 1991; Lamb et al., 2011). The loading of cobble- and boulder-mantled headwater channels with relatively fine sediment (e.g., sand and fine gravel) after a fire,

but prior to rainfall, lowers the threshold water discharge needed for the failure of channel fills during storms, leading to increased potential for debris flows (Kean et al., 2013; Prancevic et al., 2014). Rather than being driven by severe storms and soil hydrophobicity that act on hillslope soils, post-wildfire sediment yield in this model is determined by dry sediment supply, which in turn is a function of the storage capacity of sediment stored behind vegetation dams (DiBiase and Lamb, 2013; Lamb et al., 2013) and the connectivity between steep hillslopes and headwater channels (DiBiase et al., 2017). Thus, more-frequent fires may lead to less sediment yield per fire due to a supply limitation (Lamb et al., 2011), a prediction that is opposite to that of models for soil-mantled landscapes (Roering and Gerber, 2005). However, steep landscapes commonly exhibit a patchwork of soil-mantled and bare-bedrock hillslopes (DiBiase et al., 2012), making it challenging to determine the relative importance of wet versus dry transport processes.

Quantifying patterns of post-wildfire erosion and deposition on hillslopes requires high-resolution topographic surveys, and previous studies have used ground-based measurements for relatively small-scale monitoring of individual hillslopes (Tang et al., 2019), channels (Florsheim et al., 2017), or small watersheds (Kean et al., 2011; Staley et al., 2014). At larger scales, sediment yields measured from debris basins at river mouths provide constraints on the timing and magnitude of net sediment export (Lavé and Burbank, 2004; Lamb et al., 2011), but do not retain the spatial pattern of sediment sources. Repeat airborne lidar topographic surveys provide an opportunity to achieve high-resolution mapping of erosion and deposition over large areas (Pelletier and Orem, 2014; Brogan et al., 2019), but studies have yet to analyze post-wildfire, pre-rainfall data that are necessary for isolating the importance of dry sediment transport processes.

*E-mail: rdibiase@psu.edu

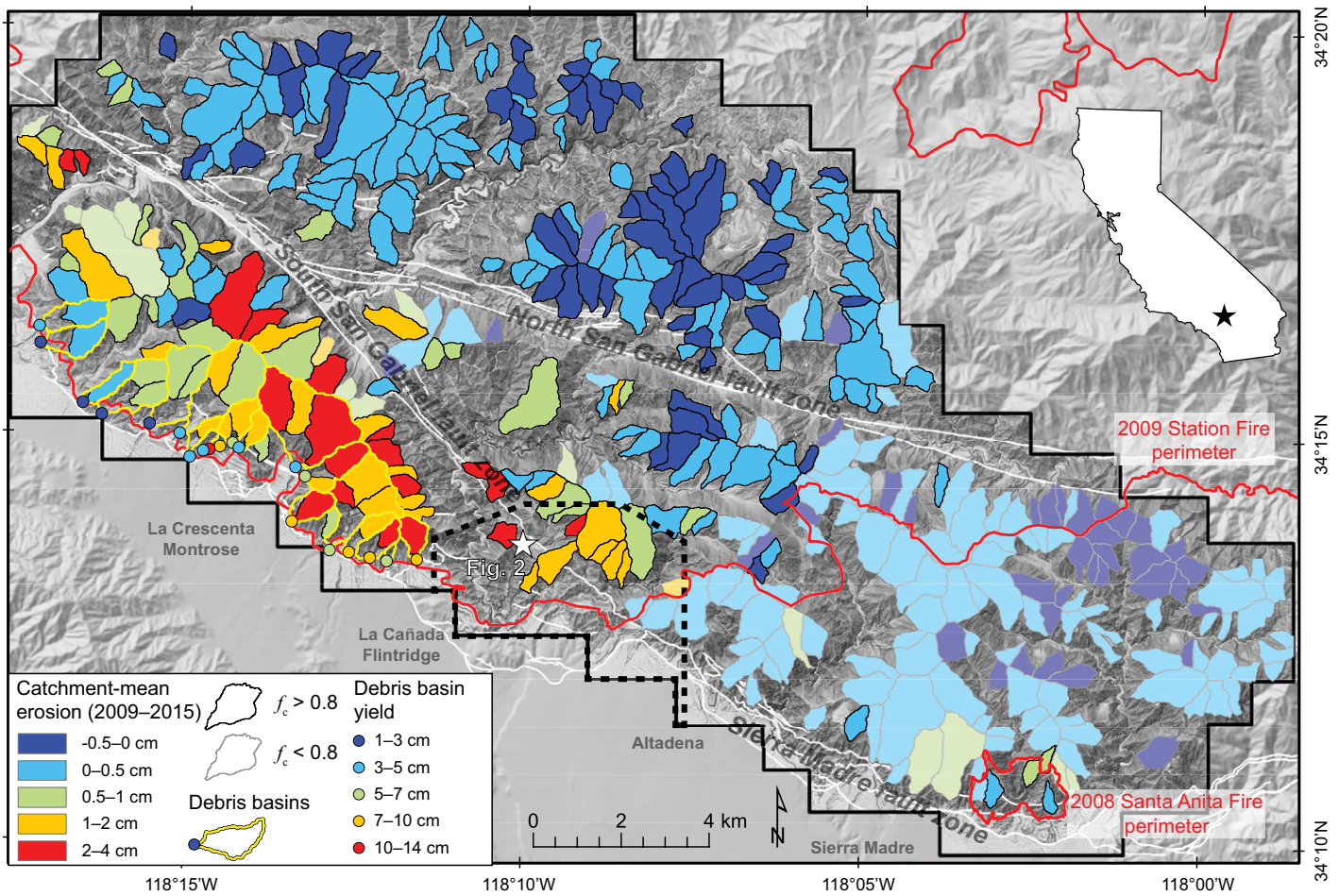


Figure 1. Overview map of the western San Gabriel Mountains, southern California, USA. Colorized polygons indicate catchment-scale airborne lidar differencing between the September 2009 and 2015–2016 surveys. Bold colors indicate catchments with high ground-shot density (fraction of channel network with data, $f_c > 0.8$) (see the Data Repository [see footnote 1]). Black outline indicates the extent of the September 2009 and 2015–2016 lidar surveys. Dashed outline indicates the extent of the June 2009 lidar survey. Red lines indicate perimeters for the 2008 Santa Anita and 2009 Station Fires. Yellow outlines indicate catchment areas for debris basins. White lines indicate Quaternary faults (<https://earthquake.usgs.gov/hazards/qfaults/>). White star indicates location of Figure 2.

Here we present repeat airborne lidar analysis of the 2009 CE Station Fire, which burned 650 km² in the steep topography of the western San Gabriel Mountains, southern California, USA (Fig. 1). The San Gabriel Mountains have served as a natural laboratory for post-wildfire debris-flow studies for decades, including pioneering work that helped develop the current understanding of dry ravel processes (e.g., Krammes, 1965), soil hydrophobicity and runoff erosion (e.g., Wells, 1987), and net sediment export into debris basins (Lavé and Burbank, 2004). In this study, we used ideally timed airborne lidar surveys to show the systematic spatial pattern of post-fire loading of headwater channels by dry ravel, and subsequent excavation of channel fills during storms.

METHODS

We used three airborne lidar surveys, conducted by the U.S. Geological Survey (<http://www.usgs.gov>) and the National Center for Airborne Laser Mapping (<http://ncalm.cive.uh.edu/>), to constrain the timing and magnitude

of landscape-scale erosional response to the 2009 Station Fire (see Table DR1 in the GSA Data Repository¹). A June 2009 lidar data set captured pre-fire topography and vegetation cover over a 15 km² region in the front range of the San Gabriel Mountains (Fig. 1). A second and more extensive data set (326 km²) was flown in September 2009, immediately following the Station Fire and prior to the first post-wildfire rainfall (Fig. 1; Fig. DR1). Where the June 2009 and September 2009 lidar data sets overlap, we quantified the topographic change associated with post-wildfire sediment loading of headwater channel networks by dry ravel. A third lidar data set was compiled from flights between September 2015 and October 2016. The difference between the 2015–2016 and September

¹GSA Data Repository item 2020054, supplementary methods, Figures DR1–DR9, Table DR1, and Watersheds.zip (shapefiles of analyzed watersheds and watershed-averaged data), is available online at <http://www.geosociety.org/datarepository/2020/>, or on request from editing@geosociety.org.

2009 data sets revealed the spatial pattern of 6–7 yr of erosion and deposition, due primarily to runoff in the wet winters of 2009–2010 and 2010–2011 (Fig. DR1).

RESULTS

The 15 km² burned region encompassed by all three lidar surveys shows a general pattern of post-wildfire loading of headwater channels with dry ravel deposits up to 3 m thick (June to September 2009 change) followed by up to 5 m of erosion in channel networks in subsequent years (September 2009 to 2015–2016 change) (Fig. 2). The observed spatial patterns of dry ravel accumulation and channel erosion are concentrated in headwater valleys with drainage areas ranging from 10³ to 10⁵ m², in agreement with predictions from a dry ravel transport model (DiBiase et al., 2017) (Fig. 2; Fig. DR2).

For 20 watersheds within our study area, post-fire sediment yields also were determined from excavation of sediment trapped in debris retention basins at catchment outlets

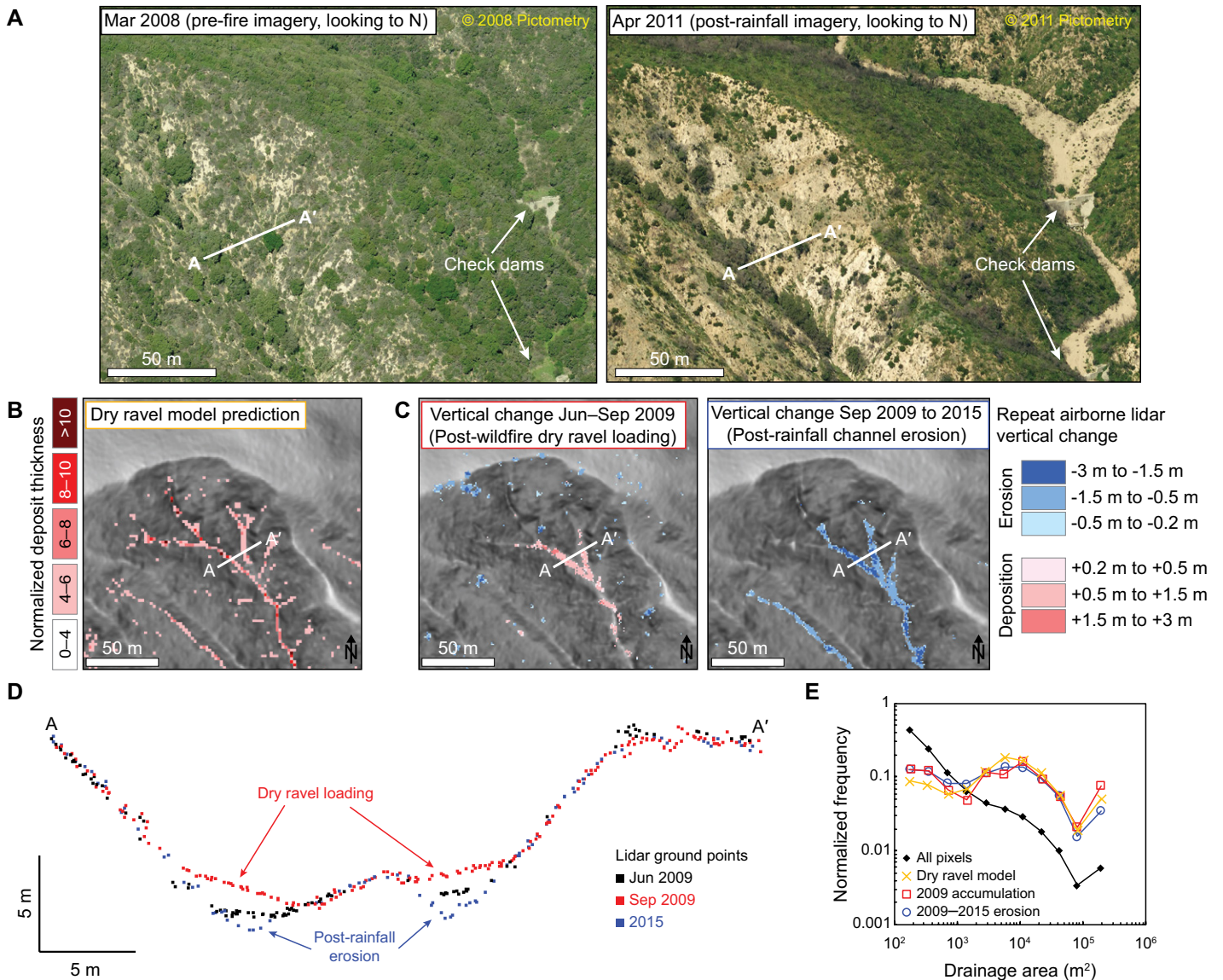


Figure 2. Landscape change predicted by the dry ravel model and resolved by airborne lidar differencing. (A) Oblique aerial imagery taken before and after the 2009 CE Station Fire near Brown Mountain, southern California, USA (white star, Fig. 1). (B) Dry ravel model prediction of post-wildfire deposition pattern. (C) Lidar-derived significant change maps showing post-wildfire dry ravel accumulation and subsequent channel erosion. (D) Cross section using lidar ground-return point cloud data showing post-fire dry ravel loading and subsequent erosion of preexisting channel deposits. (E) Drainage area frequency distributions for all pixels in the landscape (black) and predicted and observed areas of dry ravel loading and channel erosion (colors).

(Los Angeles County Department of Public Works, 2011), providing an independent comparison of our lidar-derived calculations of net channel erosion (see the Data Repository). Debris basin records indicate that most sediment was delivered in 1–2 yr following the Station Fire (equivalent to 1–14 cm of catchment-averaged lowering, and 10- to 100-fold larger than millennial erosion rates; DiBiase et al., 2010; Heimsath et al., 2012) with limited delivery during the following drought years. Lidar-derived measurements of net channel erosion averaged at the catchment scale range from 0 to 6 cm and are positively correlated with debris basin yields ($R^2 = 0.69$) (Fig. 3A). Independent estimates of pre-wildfire dry ravel storage on hill-

slopes (DiBiase and Lamb, 2013; Lamb et al., 2013) indicate nearly uniform potential for dry ravel erosion (~2 cm) for all 20 debris basin watersheds, due to similarities in vegetation cover and topography (Fig. 3A).

Topographic differencing of the September 2009 and 2015–2016 lidar data sets revealed patterns of post-wildfire channel erosion and aggradation ranging from 20 cm to >5 m, along with occasional shallow landslides on hillslopes and rockfall outside of the area burned in the 2009 Station Fire (Figs. DR3–DR5). The greatest post-wildfire erosion occurred in burned watersheds along the range front between the South San Gabriel fault zone and the Sierra Madre fault zone (Fig. 1). When averaged at the scale

of small watersheds (1–2 km²), lidar-derived calculations of net channel erosion from steep, burned watersheds are equivalent to as much as 4 cm of hillslope erosion (Fig. 1).

DISCUSSION

Our data indicate a direct connection between the loading of headwater channels with dry ravel deposits immediately following wildfire and the subsequent patterns of channel erosion due to floods and debris flows (Fig. 2). The September 2009 lidar data provide a rare snapshot of post-fire dry sediment loading in channels prior to rainfall, which is confirmed by topographic change where pre-fire lidar exists (Fig. 2C) and is identifiable in the topography

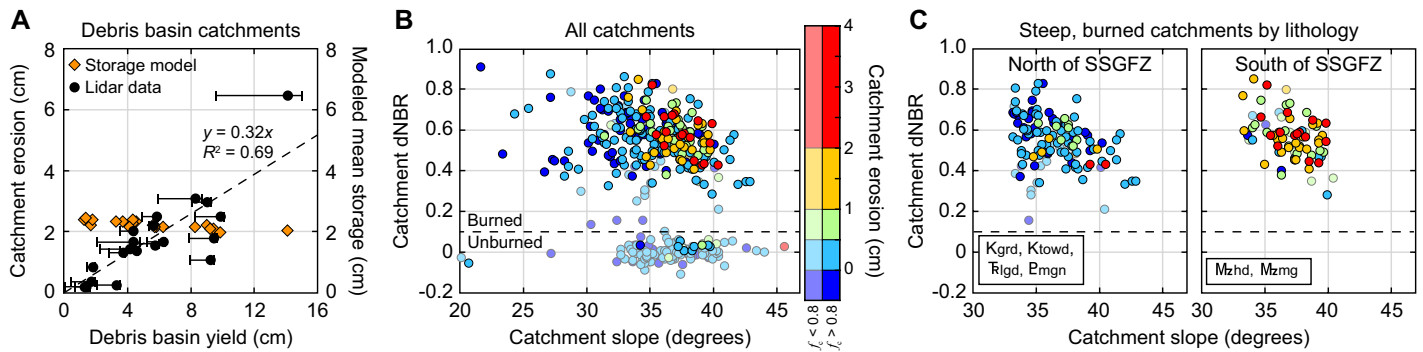


Figure 3. Catchment-scale analysis of lidar change detection. (A) 2009–2015 CE catchment erosion measured with lidar plotted against independently measured debris basin sediment yields (Fig. 1). Error bars indicate uncertainty in debris basin sediment yield (see the Data Repository [see footnote 1]). Orange diamonds indicate modeled dry ravel storage for each catchment (see the Data Repository [see footnote 1]). **(B)** Scatter plot of catchment mean difference normalized burn ratio (dNBR) and catchment mean slope for all catchments with points colorized by 2009–2015 catchment mean erosion as in Figure 1. f_c —fraction of channel network with data (see the Data Repository). **(C)** Same plot as B, showing only steep (slope $>33^\circ$) burned (dNBR >0.1) catchments separated by lithology, highlighting the correlation between higher erosion rates and highly fractured and more-mafic lithologies south of the South San Gabriel fault zone (SSGFZ). Primary lithology for each catchment is determined from Campbell et al. (2014): Kgrd, Rlgd—granodiorite; Ktowd—tonalite; Emgn—gneiss; Mzhd—hornblende diorite; Mzmg—biotite monzogranite.

as characteristic low-sloping sediment fills and debris cones (Fig. DR3). Notably, inspection of regions with limited post-wildfire erosion response shows no evidence of channel fills (Fig. DR4). We interpret the connection between dry ravel loading of channels post-fire and increased channel erosion following rainfall to reflect a hillslope sediment supply control on post-wildfire sediment yield and debris flows initiated due to dry ravel loading.

Although dry ravel loading of headwater channels leads to high post-wildfire sediment yield in our study area, our data and prior work reveal complexities in the evolution of sediment sources over time. First, there was a systematic pattern of channel erosion that exceeded dry ravel deposition (Fig. 2D), indicating the scouring of preexisting channel deposits (Santi et al., 2008). Notably, we observed this scour only in channels loaded with dry ravel following fire, suggesting that the relatively fine-grained ravel deposits helped to initiate in-channel failure as debris flows (Prancevic et al., 2014), and that these flows in turn scoured older channel fills to bedrock. Second, observations from debris-flow monitoring (Kean et al., 2011) and repeat terrestrial laser scanning (Schmidt et al., 2011; Staley et al., 2014) of a small watershed burned in the 2009 Station Fire showed a prolonged pattern of sediment supply to and evacuation of headwater channels. In addition to an initial pulse of post-wildfire dry ravel loading, the winter of 2009–2010 had extensive rainfall-driven rilling of soil-mantled hillslopes, renewed dry ravel deposition from bedrock hillslopes, and repeated evacuation of headwater channel deposits by debris flows (Kean et al., 2011; Schmidt et al., 2011; Staley et al., 2014). Because of the distributed nature of post-wildfire hillslope erosion and limitations of airborne lidar resolution, our analysis cannot capture the effects of rilling, dry

ravel, or other fine-scale hillslope erosion processes that occurred following the September 2009 lidar survey. The continued contribution of hillslope-derived sediments suggests that our lidar-derived estimates of post-wildfire erosion are likely to be minimum values and explains why lidar sediment yields are 30% of debris basin-derived sediment yields (Fig. 3A).

In general, lidar-derived post-wildfire erosion is highest for steep ($>33^\circ$) burned (difference normalized burn ratio >0.1) watersheds (Figs. 1 and 3B). However, in contrast to existing post-wildfire debris-flow models (e.g., Gartner et al., 2014) and observations in soil-mantled landscapes (Pelletier and Orem, 2014; Brogan et al., 2019), our data show no correlation between catchment slope, burn severity, and post-wildfire erosion (Fig. 3). Instead, despite similarities in topography (Fig. DR6), burn severity (Fig. DR3), fire history (Fig. DR7), and vegetation cover (Figs. DR8 and DR9), there is a strong contrast between high post-wildfire erosion along the southern range front and minimal erosional response north of the South San Gabriel fault zone (Figs. 1 and 3C). Neither vegetation storage models (DiBiase and Lamb, 2013; Lamb et al., 2013) nor a dry ravel routing model (DiBiase et al., 2017) can explain this observed pattern of post-wildfire erosion (Fig. DR6), suggesting that the difference may be related to lithology. The South San Gabriel fault zone has juxtaposed granodiorites, tonalites, and gneisses to the north with more fractured and mafic lithologies (hornblende diorite, biotite monzogranite) to the south (Campbell et al., 2014). It is possible that soil production rates are lower to the north, which caused a sediment-supply limitation, or that subtle differences in sediment size and shape or bedrock roughness made post-fire soils more stable (DiBiase et al., 2017). While future work is needed to evaluate

these hypotheses, our results support the idea that small differences in topography, sediment properties, or lithology can lead to dramatic changes in sediment yield on hillslopes that are very near the limit of sediment stability because dry ravel is inherently a threshold process.

CONCLUSIONS

Overall, our data highlight key differences in the fire-flood cycle between soil-mantled and bedrock landscapes that are important for understanding post-wildfire debris-flow hazards and longer-term landscape evolution. Rather than commonly used metrics of slope and burn severity, predicting debris-flow occurrence in bedrock landscapes requires constraining the storage, routing, and particle sizes of dry ravel, which depends on pre-fire vegetation cover, long-term sediment production rates from bedrock, and hillslope-channel connectivity (Lamb et al., 2011, 2013; DiBiase and Lamb, 2013; Prancevic et al., 2014; DiBiase et al., 2017). Beyond simply providing readily mobilized sediment, our data show how dry ravel loading of headwater channels leads to debris-flow initiation and additional scour of preexisting channel deposits during subsequent storms, which further amplifies sediment yield. In contrast, catchments without post-fire ravel accumulation in channels did not show scour during storms. Thus, the spatial pattern of dry ravel loading may largely determine post-fire sediment yield and debris-flow occurrence. While dry ravel is generally associated with steep, bedrock hillslopes, predicting the spatial pattern of loading remains a challenge. This challenge needs to be solved to determine how landscapes will respond to a changing climate with increased fire frequency because, unlike soil-mantled hillslopes, sediment yield from bedrock slopes is controlled by sediment supply. Fortunately, the accumulation of thick

sediment fills in channels immediately following fire is readily measurable by airborne lidar and allows for direct quantification of likely post-fire sediment yields and debris-flow hazards prior to rainfall.

ACKNOWLEDGMENTS

We thank Drew Decker for assistance with obtaining the June 2009 lidar data set, and Lisa Woodward for help with preliminary analysis. DiBiase acknowledges funding from the National Science Foundation (grant EAR-1848321). September 2009 lidar data were collected by the National Center for Airborne Laser Mapping with funding support from Arizona State University, the California Institute of Technology, and the U.S. Geological Survey, and are available from OpenTopography (<https://doi.org/10.5069/G94M92N4>). Comments from Tom Dunne and two anonymous reviewers helped improve the paper.

REFERENCES CITED

- Brogan, D.J., Nelson, P.A., and MacDonald, L.H., 2019, Spatial and temporal patterns of sediment storage and erosion following a wildfire and extreme flood: *Earth Surface Dynamics*, v. 7, p. 563–590, <https://doi.org/10.5194/esurf-7-563-2019>.
- Campbell, R.H., Wills, C.J., Irvine, P.J., and Swanson, B.J., compilers, 2014, Preliminary geologic map of the Los Angeles 30' × 60' quadrangle, California, version 2.1: Sacramento, California Geological Survey, 1 sheet, scale 1:100,000, 119 p. text.
- Cannon, S.H., and DeGraff, J., 2009, The increasing wildfire and post-fire debris-flow threat in western USA, and implications for consequences of climate change, in Sassa, K., and Canuti, P., eds., *Landslides—Disaster Risk Reduction*: Berlin, Springer, p. 177–190, https://doi.org/10.1007/978-3-540-69970-5_9.
- DiBiase, R.A., and Lamb, M.P., 2013, Vegetation and wildfire controls on sediment yield in bedrock landscapes: *Geophysical Research Letters*, v. 40, p. 1093–1097, <https://doi.org/10.1002/grl.50277>.
- DiBiase, R.A., Whipple, K.X., Heimsath, A.M., and Ouimet, W.B., 2010, Landscape form and millennial erosion rates in the San Gabriel Mountains, CA: *Earth and Planetary Science Letters*, v. 289, p. 134–144, <https://doi.org/10.1016/j.epsl.2009.10.036>.
- DiBiase, R.A., Heimsath, A.M., and Whipple, K.X., 2012, Hillslope response to tectonic forcing in threshold landscapes: *Earth Surface Processes and Landforms*, v. 37, p. 855–865, <https://doi.org/10.1002/esp.3205>.
- DiBiase, R.A., Lamb, M.P., Ganti, V., and Booth, A.M., 2017, Slope, grain size, and roughness controls on dry sediment transport and storage on steep hillslopes: *Journal of Geophysical Research: Earth Surface*, v. 122, p. 941–960, <https://doi.org/10.1002/2016JF003970>.
- Doerr, S.H., Shakesby, R.A., and MacDonald, L.H., 2009, Soil water repellency: A key factor in post-fire erosion, in Cerdá, A., and Robichaud, P.R., eds., *Fire Effects on Soils and Restoration Strategies*: Boca Raton, Florida, CRC Press, p. 197–223.
- Florsheim, J.L., Keller, E.A., and Best, D.W., 1991, Fluvial sediment transport in response to moderate storm flows following chaparral wildfire, Ventura County, southern California: *Geological Society of America Bulletin*, v. 103, p. 504–511, [https://doi.org/10.1130/0016-7606\(1991\)103<0504:FS TIRT>2.3.CO;2](https://doi.org/10.1130/0016-7606(1991)103<0504:FS TIRT>2.3.CO;2).
- Florsheim, J.L., Chin, A., Kinoshita, A.M., and Nourbakhshbeidokhti, S., 2017, Effect of storms during drought on post-wildfire recovery of channel sediment dynamics and habitat in the southern California chaparral, USA: *Earth Surface Processes and Landforms*, v. 42, p. 1482–1492, <https://doi.org/10.1002/esp.4117>.
- Gabet, E.J., 2003, Post-fire thin debris flows: Sediment transport and numerical modelling: *Earth Surface Processes and Landforms*, v. 28, p. 1341–1348, <https://doi.org/10.1002/esp.590>.
- Gartner, J.E., Cannon, S.H., and Santi, P.M., 2014, Empirical models for predicting volumes of sediment deposited by debris flows and sediment-laden floods in the transverse ranges of southern California: *Engineering Geology*, v. 176, p. 45–56, <https://doi.org/10.1016/j.enggeo.2014.04.008>.
- Heimsath, A.M., DiBiase, R.A., and Whipple, K.X., 2012, Soil production limits and the transition to bedrock-dominated landscapes: *Nature Geoscience*, v. 5, p. 210–214, <https://doi.org/10.1038/ngeo1380>.
- Kean, J.W., Staley, D.M., and Cannon, S.H., 2011, In situ measurements of post-fire debris flows in southern California: Comparisons of the timing and magnitude of 24 debris-flow events with rainfall and soil moisture conditions: *Journal of Geophysical Research*, v. 116, F04019, <https://doi.org/10.1029/2011JF002005>.
- Kean, J.W., McCoy, S.W., Tucker, G.E., Staley, D.M., and Coe, J.A., 2013, Runoff-generated debris flows: Observations and modeling of surge initiation, magnitude, and frequency: *Journal of Geophysical Research: Earth Surface*, v. 118, p. 2190–2207, <https://doi.org/10.1002/jgrf.20148>.
- Krammes, J.S., 1965, Seasonal debris movement from steep mountainside slopes in southern California, in *Proceedings of the Second Federal Interagency Sedimentation Conference*: Washington, D.C., U.S. Department of Agriculture, p. 85–89.
- Lamb, M.P., Scheingross, J.S., Amidon, W.H., Swanson, E., and Limaye, A., 2011, A model for fire-induced sediment yield by dry ravel in steep landscapes: *Journal of Geophysical Research*, v. 116, F03006, <https://doi.org/10.1029/2010JF001878>.
- Lamb, M.P., Levina, M., DiBiase, R.A., and Fuller, B.M., 2013, Sediment storage by vegetation in steep bedrock landscapes: Theory, experiments, and implications for postfire sediment yield: *Journal of Geophysical Research: Earth Surface*, v. 118, p. 1147–1160, <https://doi.org/10.1002/jgrf.20058>.
- Lavé, J., and Burbank, D., 2004, Denudation processes and rates in the Transverse Ranges, southern California: Erosional response of a transitional landscape to external and anthropogenic forcing: *Journal of Geophysical Research*, v. 109, F01006, <https://doi.org/10.1029/2003jf000023>.
- Los Angeles County Department of Public Works, 2011, Hydrologic report 2009–2010: Alhambra, California, County of Los Angeles Department of Public Works, Water Resources Division, 531 p., <http://www.ladpw.org/wrd/report/> (accessed July 2019).
- Mann, M.L., Batllori, E., Moritz, M.A., Waller, E.K., Berck, P., Flint, A.L., Flint, L.E., and Dolfi, E., 2016, Incorporating anthropogenic influences into fire probability models: Effects of human activity and climate change on fire activity in California: *PLoS One*, v. 11, e0153589, <https://doi.org/10.1371/journal.pone.0153589>.
- Moody, J.A., Shakesby, R.A., Robichaud, P.R., Cannon, S.H., and Martin, D.A., 2013, Current research issues related to post-wildfire runoff and erosion processes: *Earth-Science Reviews*, v. 122, p. 10–37, <https://doi.org/10.1016/j.earscirev.2013.03.004>.
- Parsons, A., Robichaud, P.R., Lewis, S.A., Napper, C., and Clark, J.T., 2010, Field guide for mapping post-fire soil burn severity: U.S. Department of Agriculture, Forest Service, Rocky Mountain Research Station General Technical Report RMRS-GTR-243: 49 p., <https://doi.org/10.2737/RMRS-GTR-243>.
- Pelletier, J.D., and Orem, C.A., 2014, How do sediment yields from post-wildfire debris-laden flows depend on terrain slope, soil burn severity class, and drainage basin area? Insights from airborne-LiDAR change detection: *Earth Surface Processes and Landforms*, v. 39, p. 1822–1832, <https://doi.org/10.1002/esp.3570>.
- Prancevic, J.P., Lamb, M.P., and Fuller, B.M., 2014, Incipient sediment motion across the river to debris-flow transition: *Geology*, v. 42, p. 191–194, <https://doi.org/10.1130/G34927.1>.
- Roering, J.J., and Gerber, M., 2005, Fire and the evolution of steep, soil-mantled landscapes: *Geology*, v. 33, p. 349–352, <https://doi.org/10.1130/G21260.1>.
- Santi, P.M., deWolfe, V.G., Higgins, J.D., Cannon, S.H., and Gartner, J.E., 2008, Sources of debris flow material in burned areas: *Geomorphology*, v. 96, p. 310–321, <https://doi.org/10.1016/j.geomorph.2007.02.022>.
- Schmidt, K.M., Hanshaw, M.N., Howle, J.F., Kean, J.W., Staley, D.M., Stock, J.D., and Bawdeng W., W., 2011, Hydrologic conditions and terrestrial laser scanning of post-fire debris flows in the San Gabriel Mountains, CA, U.S.A. in *Proceedings of the Fifth International Conference on Debris Flow Hazards Mitigation: Mechanics, Prediction, and Assessment*, Padua, Italy, 14–17 June 2011: Rome, Casa Editrice Università La Sapienza, p. 583–593, <https://doi.org/10.4408/IJEGE.2011-03.B-064>.
- Staley, D.M., Wasklewicz, T.A., and Kean, J.W., 2014, Characterizing the primary material sources and dominant erosional processes for post-fire debris-flow initiation in a headwater basin using multi-temporal terrestrial laser scanning data: *Geomorphology*, v. 214, p. 324–338, <https://doi.org/10.1016/j.geomorph.2014.02.015>.
- Tang, H., McGuire, L.A., Rengers, F.K., Kean, J.W., Staley, D.M., and Smith, J.B., 2019, Evolution of debris-flow initiation mechanisms and sediment sources during a sequence of post-wildfire rainstorms: *Journal of Geophysical Research: Earth Surface*, v. 124, p. 1572–1595, <https://doi.org/10.1029/2018JF004837>.
- Wells, W.G., 1987, The effects of fire on the generation of debris flows in southern California: *Reviews in Engineering Geology*, v. 7, p. 105–114, <https://doi.org/10.1130/REG7-p105>.
- Westerling, A.L., and Bryant, B.P., 2008, Climate change and wildfire in California: *Climatic Change*, v. 87, no. S1, p. 231–249, <https://doi.org/10.1007/s10584-007-9363-z>.

Printed in USA